

1

2 *G-Cubed*

3

Supporting Information for

4

**The Earth's hum variations from a global model and seismic recordings  
around the Indian Ocean**

6

M. Deen<sup>1</sup>, E. Stutzmann<sup>1</sup>, F. Ardhuin<sup>2,3</sup>

7

<sup>1</sup>Institut de Physique du Globe, de Paris, Sorbonne Paris Cite, UMR7154 CNRS, Paris, France

8

<sup>2</sup>Ifremer, Laboratoire d'Océanographie Spatiale, Brest, France

9

<sup>3</sup>Laboratoire de Physique des Oceans, CNRS-Ifremer-UBO-IRD, Brest, France

10

11

12

13 **Contents of this file**

14

15 Text S1

16

Figures S1 to S2

17

Captions for Movies S1

18

19 **Additional Supporting Information (Files uploaded separately)**

20

21

Movies S1

22

23 **Introduction**

24

The supporting information includes a movie that shows the influence of local storms on the hum signal recorded by the 4 stations that were used in the main text. In this text file we show the results of 3 seismic stations as an extended work to the data used in the main text.

27

28

29

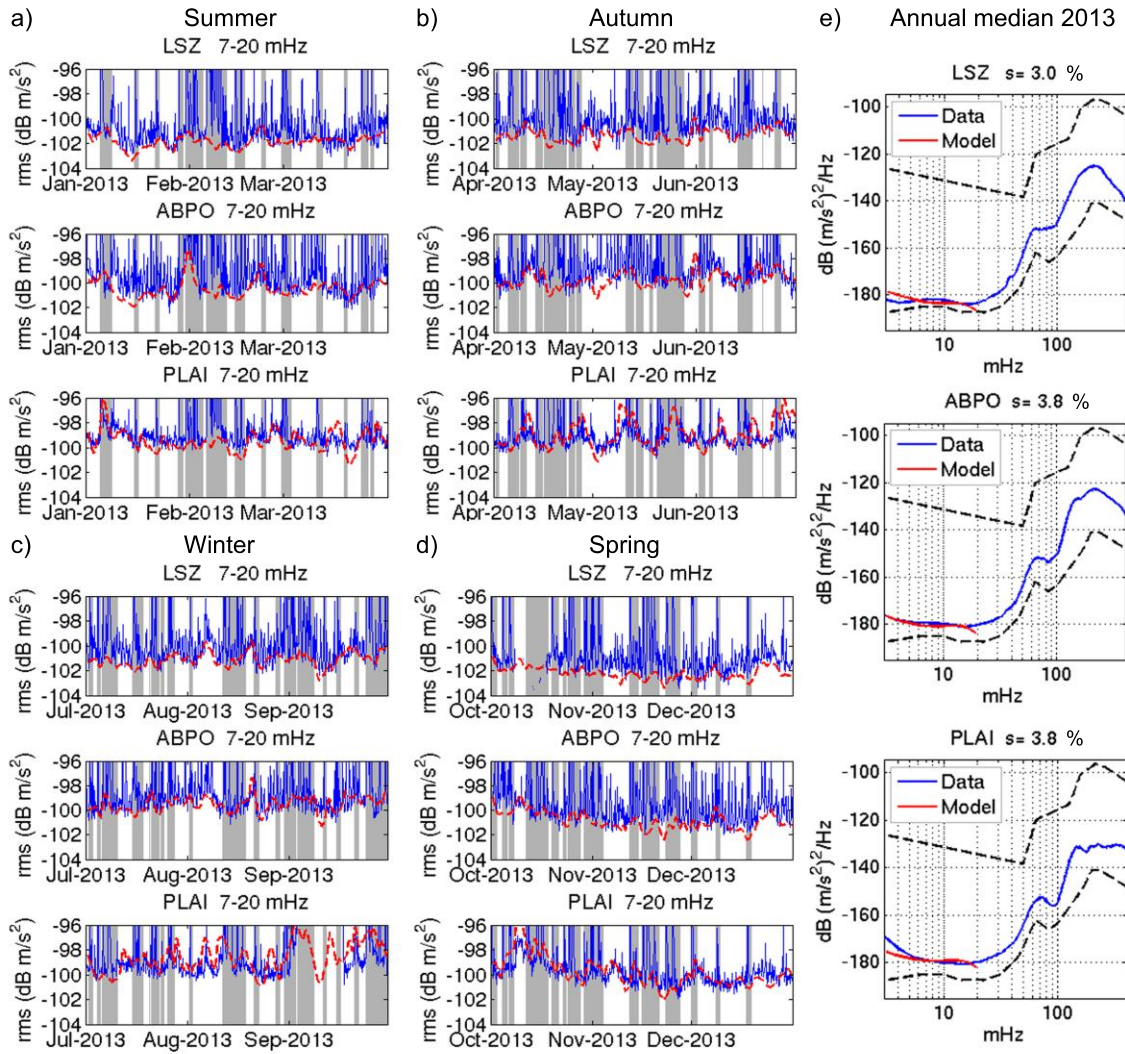
30

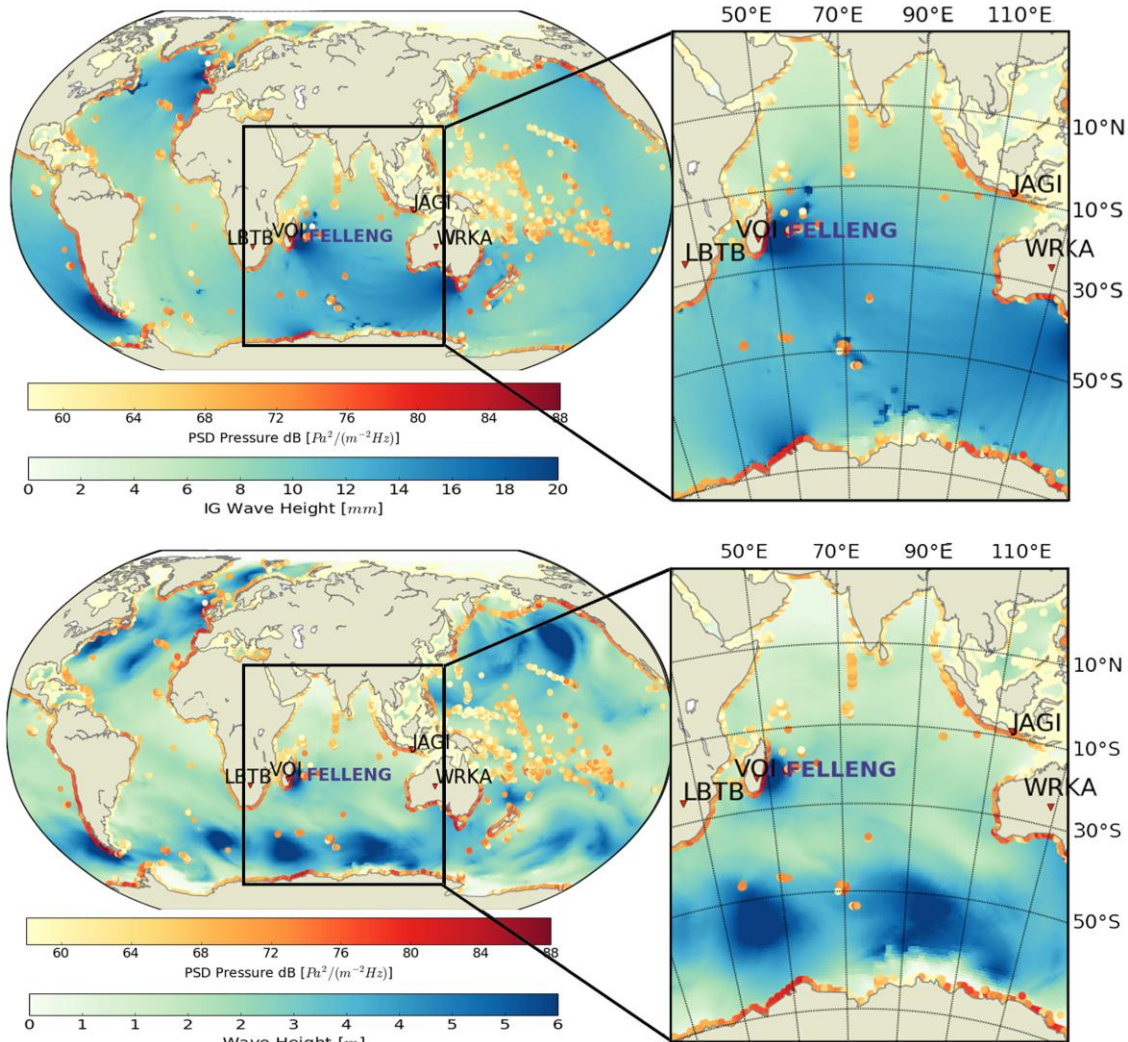
31 **Text S1.**  
32 We show the observed and modeled seismic PSD for 3 other stations: LSZ in Zimbabwe,  
33 ABPO in Madagascar and PLAI in Indonesia. The stations follow similar temporal trends  
34 as do their neighboring stations LBTB, VOI and JAGI respectively. We show the results  
35 in figure S1. Station ABPO (b) follows a similar trend to VOI in figure 3 the main text,  
36 and shows an equal increase in RMS amplitude as VOI. LSZ (a) follows a similar trend  
37 as LBTB in figure 4 of the main text; and PLAI follows a similar trend as WRKA in  
38 figure 4 of the main text.  
39  
40 Figure S2 compares infragravity wave height (top) to swell waveheight (bottom) at the  
41 time of cyclone Felleng as shown in the bottom plot of figure 4 in the main text. The  
42 infragravity wave height is parameterized at the coast from the swell wave height  
43 multiplied with the mean period and the square root of gravity divided by water depth  
44 (Ardhuin et al, 2014). Afterwards the IG wave heights are extrapolated for the deep  
45 ocean. At the coasts we see similar patterns for both wave heights. In the deep ocean the  
46 waveheights show different patterns, because the swell wave height is calculated from  
47 local winds; and the free infragravity waveheight is propagated from the coast.  
48  
49

50

51 **Figure S1.** (a-d): Comparison between data (blue) and synthetic (red) RMS amplitudes of  
 52 the vertical acceleration averaged between 7 and 20 mHz as in figure 3, but with different  
 53 stations: LSZ, ABPO, PLAI. The station locations are in figure 2 of the main text in light grey.  
 54 The times of earthquakes are shows in grey, coinciding with an increase in spectral amplitude in  
 55 blue. (e) displays the median data in blue and median model in red; and the slope factor  $s$   
 56 required to fit the two. The black dashed lines represent the low and high noise level of  
 57 (Peterson, 1993).

58





59

60 **Figure S2.** Infragravity wave height in mm (top) and swell wave height in m (bottom) and PSD  
 61 pressure sources in similar to figure 4 of the main text. The infragravity wave height in mm is  
 62 calculated following Ardhuin et al. (2014).

63

64 **Movie S1.** Global time lapse of storms (in purple) with infragravity waveheight (in blue  
 65 colorscale [mm]) and hum pressure sources (in red colorscale [dB of pressure]). Station  
 66 locations and names are indicated with red triangles and black letters respectively. In the  
 67 bottom are the recorded (blue) and modeled (red) rms in dB of seismic acceleration at 4  
 68 stations (LBTB, VOI, JAGI and WRKA) between 7 and 20 mHz. The red dot indicates the point in  
 69 time corresponding to the top figure.

70

71